



Indian Journal of Engineering & Materials Sciences
Vol. 27, April 2020, pp. 404-409



Microstructure, texture, and mechanical properties of two-pass extruded Mg-5Li-1Al sheet

Ruihong Li^{a*}, Bin Jiang^b, Zhijun Chen^c, Fusheng Pan^b, Xiaomei Zhang^d

^a School of Materials and Metallurgy, Inner Mongolia University of Science and Technology, 7 Arden Street, Baotou 014010, China

^b College of Materials Science and Engineering, Chongqing University, Chongqing 400044, China

^c The tenth sub-company, Inner Mongolia First Machinery Group Corporation, Baotou 014030, China

^d Quality Management Department, Inner Mongolia First Machinery Group corporation, Baotou 014030, China

Received: 09 February 2017; Accepted: 23 December 2019

To overcome the difficult deformation of common Mg alloys, the Mg-5Li-1Al (wt %) alloy sheet with good strength-ductility balance has been successfully fabricated by two-pass extrusion at 280 °C. The microstructural evolution, texture, mechanical properties and stretch formability of the extruded sheets have been investigated. The results show that a refined microstructure can be obtained by two-pass extrusion due to dynamic recrystallization (DRX). The extruded sheet exhibits excellent formability with elongation to failure (FE) of 34% and Erichsen value of 4.82. The superior mechanical properties have been owing to both ultrafine DRX grains and weaken basal texture resulted from lithium addition.

Keywords: Mg-Li alloy, Formability, Texture, Ductility, Extrusion

1 Introduction

Magnesium and its alloys, acting as the lightest construction metals in the automotive, aerospace, and electronic industries, have been given considerable attention due to their low density, good castability, and excellent comprehensive properties¹⁻⁴. However, the insufficient number of operative slip in the hexagonal close-packed (hcp) structure limits the applications of wrought magnesium alloys^{5,6}. Generally, the strong crystallographic texture is observed in this structure, namely the basal (0001) planes of vast majority of grains close to the sheet planes⁷⁻¹⁰, hence the deformation of common magnesium alloy is relatively difficult at room temperature.

Several studies were devoted to alleviate the basal texture in magnesium alloy sheets through alloying and thermo-mechanical processing¹⁰⁻¹³. Light rare earth metals have been widely used to control the texture, such as cerium or neodymium. But the cost of these Mg alloys is higher and the preparation is more difficult than common Mg alloys¹⁴⁻¹⁶. The addition of Lithium can make Mg alloy attractive because it is an ultralight alloy with higher specific strength. The lithium addition also can improve the room-temperature ductility of Mg¹⁷⁻²¹. A number of studies

explored that Li addition can improve activities of cross-slip and non-basal slip systems in α -Mg phase, which make Mg-Li alloys have better plastic deformation ability²². However, Mg-Li alloys suffer from the lower strength. The third element, such as Al, Zn, and Ag, is often simultaneously added into Mg-Li alloys for improving the strength by good solid solution strengthening effect^{2, 21, 23-25}.

Although a large number of related reports mainly focus on the microstructure and mechanical properties of Mg-Li alloys, there are few reports on the investigation about improving the mechanical property and stretch formability of Mg-Li-Al alloys through two-pass extrusion, as well as induced recrystallization behavior. In this work, the microstructure and mechanical property of two-pass extruded Mg-5Li-1Al alloy sheet were investigated. In addition, the texture evolution during two-pass extrusion are discussed in detail, and the formability are also analyzed.

2 Experimental Procedure

The Mg-5Li-1Al (LA51) alloy used in the experiment was cast in a vacuum electromagnetic induction furnace under an argon atmosphere. The material of Mg, Li, and Al is commercially pure (>99.9%). The melt was held at 700 °C for 20 min and then poured into a metallic die with diameter of

*Corresponding author (E-mail: li Ruihong1019@163.com)

85 mm and length of 450 mm under protective atmosphere of argon gas. The cast billets were homogenizing treated at 280 °C for 24 h and then followed under air cooling condition. Afterward, the homogenized ingot was extruded firstly at 280 °C to get a rod with size of diameter 80 mm. Then the rod was extruded secondly at 280 °C to obtain a sheet with thickness of 1mm and width of 56 mm. Between two pass extrusion, the rod was annealed at 220 °C for 30 min. The actual measured chemical composition of the as-cast alloy was Mg-4.72Li-0.98Al (wt%), which was determined by inductively coupled plasma atomic emission spectrometer.

To reveal the microstructure, the samples were sectioned, mounted and polished, followed by etching 1-5 s in the etchant of 5 g picric acid, 10 ml acetic acid, and 95 ml ethyl alcohol. The optical microscopy (OM) and scanning electron microscopy (SEM) were used to observe the microstructure of the specimen. Phase analysis was performed by RIGAKU D/MAX 2500PC X-ray diffractometry (XRD). The texture and crystallographic orientation were analyzed by electron backscattered diffraction (EBSD). In order to remove surface strain, the piece was mechanically ground and electro-chemically polished at 20V and -15 °C for ~60 s. The data was analyzed with the HKL Channel 5 EBSD software and it was not considered that the misorientations were lower than 0.5° in the data post-processing. A 15 ° criterion was employed to differentiate high-angle grain boundaries (HAGBs) and low-angle grain boundaries (LAGBs). The accompanied sub-grains were defined by boundaries with mis-orientation larger than 2°.

The mechanical properties were measured by uniaxial tensile test at a strain rate of 3mm min⁻¹ at room temperature. The tensile specimens of the as-extruded plates were cut into flat along the extruding direction (ED), transverse direction (TD), and 45° from ED, with a gauge section of 25 mm×10 mm×1mm. In order to further quantify strain hardening behaviour of the two-pass extruded LA51 alloy, the uniform plastic deformation stage in uniaxial tensile curve is calculated by the equation²⁶:

$$\sigma = K\varepsilon_p^n \quad \dots (1)$$

where K , ε_p and n represent the strength coefficient, true plastic strain, and the strain hardening exponent, respectively. The stretch formability of two-pass extruded LA51 sheet was investigated by Erichsen test on a circular blank with a diameter of 50 mm,

using a hemispherical punch with a diameter of 20 mm at room temperature. Blank-holder force and the punch speed were 10 kN and 6 mm/min, respectively. The Erichsen value was obtained during Erichsen test. Graphite grease was used as a lubricant on the central part of the specimens.

3 Results and Discussion

XRD patterns of as-cast LA51 and the two-pass extruded LA51 alloy are shown in Fig. 1. The strong peaks of α -Mg phase are detected in the two alloys, and new phases are not found after two-pass extrusion.

Figure 2 (a) and (b) shows the microstructure of as-cast and two-pass extruded LA51 alloys. It reveals that the equiaxed grains distribute in as-cast LA51 alloy, and the average grain size is about 230 μm . After two-pass extrusion, the specimen exhibits homogeneous microstructure with fine equiaxed grains due to dynamic recrystallization (DRX). The SEM images of both alloys are shown in Fig. 2 (c) and (d). It is noticed that there are a small amount of particles distributing in the as-cast LA51 alloy matrix. After two-pass extrusion, the particles are broken down into tiny granulated phases distributing along the ED. Because Li element cannot be detected by EDS, the particles cannot be identified by AlLi phases. Besides, according to XRD results, there are no new phases in as-cast and extruded LA51 alloy, thus these particles may be inclusions or Mg-Al-Li second phases.

To examine grain size and texture of the two-pass extruded LA51 sheet exactly, EBSD analyses were conducted, and the results are shown in Fig. 3. The different colours represent the orientations of the

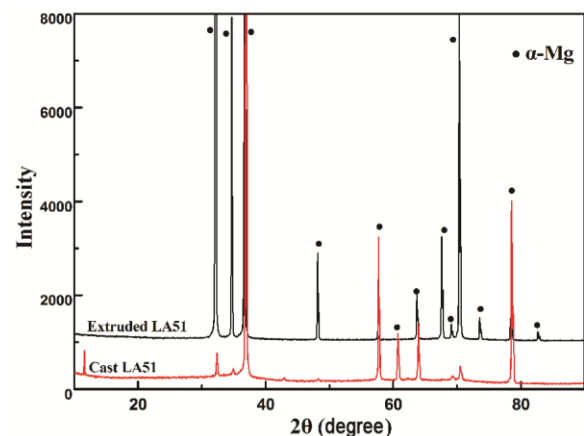


Fig.1 — XRD pattern of as-cast LA51 alloy (a) two-pass extruded LA51 sheet (b)

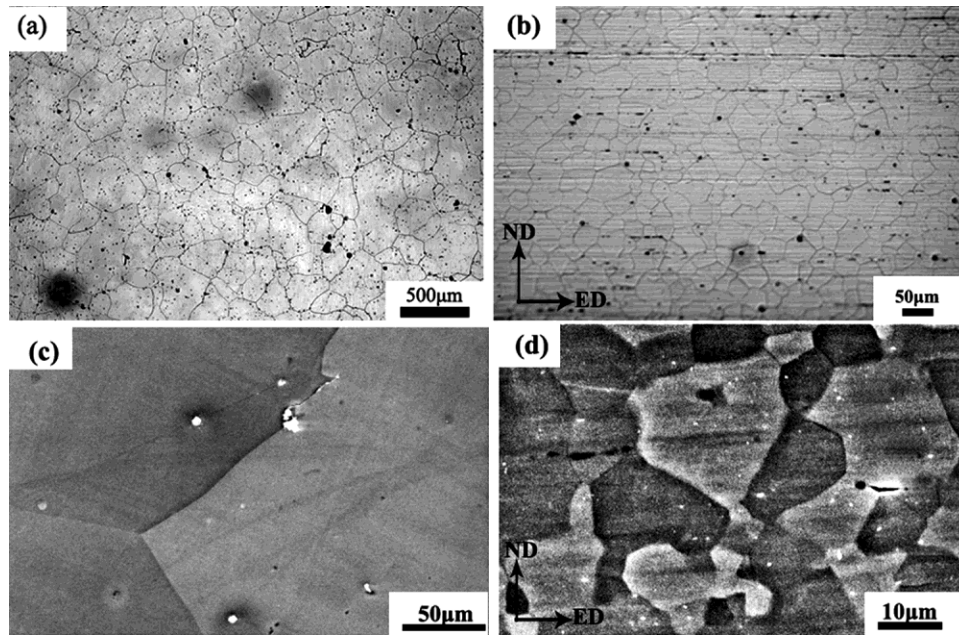


Fig. 2 — Microstructures of as-cast (a, c) and two-pass extruded Mg-5Li-1Al alloy (b, d)

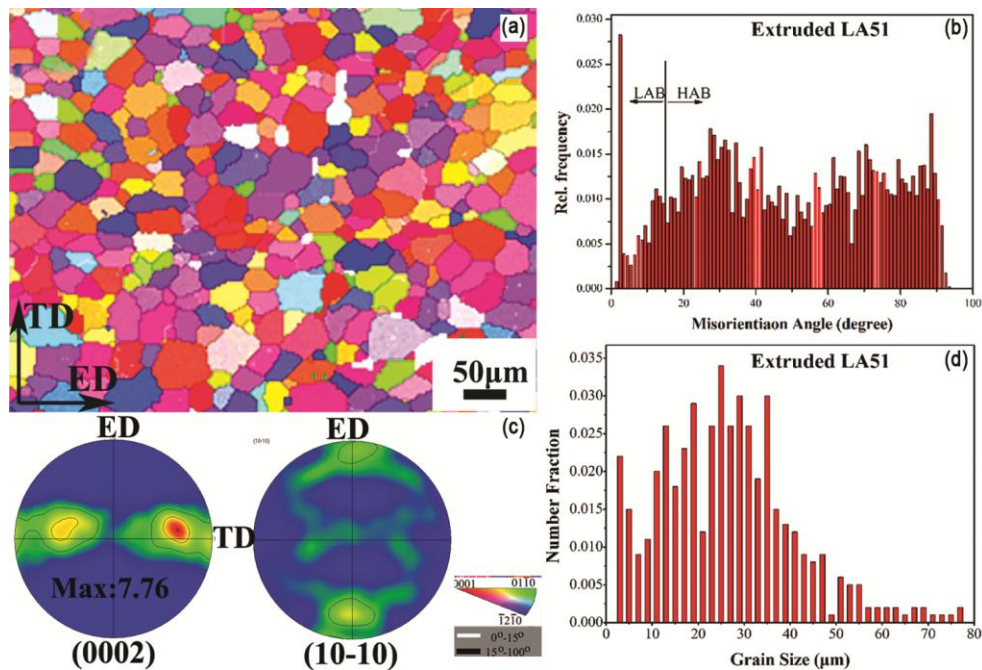


Fig. 3 — EBSD map (a) misorientation angle distribution, (b) IPF, (c) distribution of grain size and (d) taken in the two-pass extruded LA51 sheet.

respective grains. Red color indicated (0002) basal plane parallel with the sheet plane while blue color represented (0002) planes lying 90° away from the sheet plane. Meanwhile, HAGBs with misorientation angles larger than 15° and LAGBs with misorientation angles of 2° - 15° were indicated by black and white lines, respectively. It reveals that the two-pass textured

LA51 alloy had relatively weak (0002) texture, which is quite different with common Mg sheet⁸, while the basal poles of most grains rotate toward TD in the present LA51 sheet. Besides, after two-pass extrusion, the LA51 sheet shows large frequency of HAGBs, meaning more random distribution of grains. The average grain size was about $25\mu\text{m}$.

It is suggested that the weaken basal texture of the two-pass extruded LA51 sheet was originated from the random distribution of grain, on account of two pass extrusion and the decreased axial ratio (*c/a*) due to Li addition. The *c/a* is known to have great influence on the deformation mechanism. Reduced *c/a* ratio of Mg alloy enhanced the activity of prismatic $\langle a \rangle$ slip and pyramidal $\langle c+a \rangle$ slip mode²⁷. It has been observed that slip of non-basal $\langle c+a \rangle$ type dislocation is also promoted by adding lithium²². As a result, the weaker basal texture is attributed to Li addition due to the prismatic or pyramidal slip. It is discussed that prismatic slip mode had effect on the grains with their basal poles rotate toward the TD²⁸. In this work, it is further confirmed that lithium addition produced a considerable reduction in basal texture intensity with the basal pole spreading toward TD (Fig. 3). According to the report²⁹, a plane-strain compression texture was found in a hot strip-extruded Mg-4.6 wt% Li alloy, which was similar to that of metals characterized by significant prismatic slip, like Ti and Zr.

Figure 4 displays the tensile stress-strain curves of the two-pass extruded LA51 sheets evaluated along ED, TD, and 45° from ED. The 0.2% proof stress (YS), ultimate tensile strength (UTS) and elongation to failure (FE) also are summarized in Table 1. The tensile properties of a cast-rolled LA51 sheet² are also shown in Table 1 in comparison with the previous work. As can be seen that both the FE and *n* value of the “45°” sample show the highest while the UTS and YS are reverse. The FE values of the extruded LA51 sheet at all direction show larger than those of the rolled LA51 sheet. The maximum FE of 33.9% is achieved in the “45°” sample, while that of the rolled LA51 is no more than 25%². As shown above, the mechanical behaviors during tensile tests were strongly affected by the basal pole splitting toward the TD. Meanwhile, it is proved from Fig.3 that the two-pass extruded LA51 alloy exhibited greater spreading of the basal poles toward the TD than the RD. Therefore, a planar mechanical anisotropy was observed in the two-

pass extruded LA51 alloy. In the conventional magnesium alloy, Schmidt factor (SF) is calculated by³⁰:

$$SF = \cos \Phi \cdot \cos \lambda \quad \dots (2)$$

Where Φ is the angle of tensile direction with respect to the normal direction of slip plane, and λ is the angle between tensile direction and optimal slip direction. In the two-pass extruded LA51 alloy of this work, Φ of “TD” samples are mainly about 50°, while the same value of the “45°” sample and the “ED” sample are about 60° and 80-100° (Fig. 3(c)), respectively. Therefore, the SF of basal plane for “TD” sample and “45°” sample are about 0.5 and 0.45, respectively. At the same time, the SF of basal plane for “ED” sample is smaller than 0.17. As a result, the basal slip is more effective for the “TD” sample and the “45°” sample, which is beneficial to plastic deformation. On the other hand, the activity of basal slip is limited because of the small SF for the “ED” sample. Therefore, the yield strength of the “ED” sample is the highest among all the alloys.

In general, the activation of slip systems in Mg alloys strongly effected by the critical resolved shear

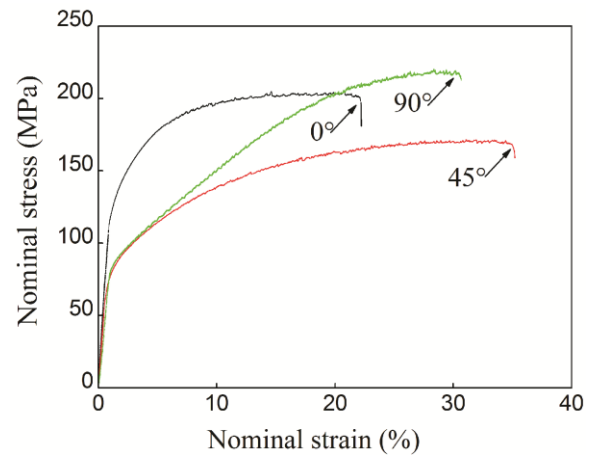


Fig. 4 — Nominal strain-stress curve of the two-pass extruded LA51 sheet tested at room temperature.

Table 1 — Mechanical properties of the two-pass extruded LA51 sheet.

Sample	Orientation	UTS(MPa)	YS(MPa)	Yield ratio	FE(%)	<i>n</i>
two-pass extruded LA51	ED	199	121	0.61	22.4	0.233
	45°	171	92	0.54	33.9	0.360
	TD	220	93	0.42	29.9	0.292
As-rolled LA51 ²	RD	140	68	0.49	19.2	—
	TD	142	68	0.48	24.1	—

stress (CRSS). It is widely believed that CRSS values for slip systems in Mg alloys are: $CRSS_{\text{basal slip}} < CRSS_{\text{prismatic slip}} < CRSS_{\text{pyramidal slip}}$ ³¹. Basal slip is an crucial slip mode in common Mg alloy probably due to its low CRSS. Non-basal slip is hardly activated as it has a larger CRSS compared to basal slip. In fact, the formability of Mg alloys is improved with Li addition, which can be attributed to the activation of the prismatic slip and pyramidal slip at temperatures below 200 °C. Li addition can effectively reduce both the dislocation energy of Mg and the CRSS for non-basal slip. Therefore, pyramidal slip tend to play an important role in plastic deformation, which largely improved formability and rolling ability of Mg-Li sheet. Moreover, it is interesting that the texture did not have much effect on UTS of the two-pass extruded LA51 sheet, which is in accord with the result in reference³².

Stretch formability of the two-pass extruded LA51 sheet at room temperature is investigated by conical cup tests. The result is shown in Fig. 5. The two-pass extruded LA51 sheet exhibits a good Stretch formability (the Erichsen values with 4.82 mm from Fig.5 (b)), which is larger than that of the hot-rolled AZ31 alloy (4.7 mm)³³. As is known, the Erichsen values of most magnesium alloy sheets at room temperature are no larger than 4.0 mm³⁴. Note that the Li addition plays a great role for the stretch formability of the LA51 sheet. Top view of the extruded LA51 sheet after Erichsen test is indicated in Fig.5 (a). The surface crack paralleling to ED appeared in all extruded LA51 sheets. However, there are several reports showed that, during Erichsen tests surface crack paralleling to the RD was observed in rolled AZ31 Mg sheet, which had a basal texture with basal pole splitting towards the RD. This result indicates the non-basal texture with basal pole rotating toward the TD had a very important impact on the macroscopic fracture behavior of the two-pass extruded LA51 sheet during Erichsen tests.

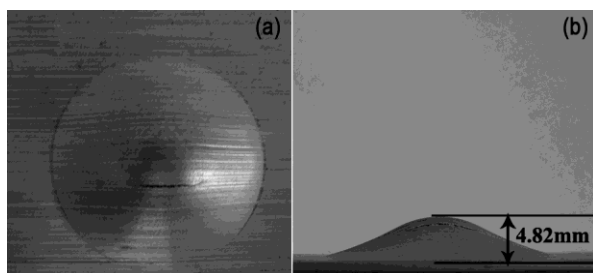


Fig. 5 — Deformed specimen after the Erichsen tests of the two-pass extruded LA51 sheets at room temperature.

It is also known that stretch formability is related to the strain-hardening exponent (n-value). Larger n-value usually means better ductility, especially uniform FE at room temperature. Both steel and Al alloys have n-values of about 0.2~0.5 at room temperature, but the n-values of common Mg alloys are smaller than 0.2. For instance, n values of AM30 and AZ31 alloy sheets were 0.17 and 0.14, respectively³⁵. Nevertheless, the present LA51 sheets display larger n-values ranging from 0.233 to 0.360 (see Table 1). In addition, during plastic deformation there is another criterion which materials can sustain the work hardening that is yield ratio³⁶. The lower the yield ratio, the better the stretch formability. The yield ratios of the two-pass extruded LA51 alloy in three directions are smaller than 0.7. Therefore, the good stretch formability of two-pass extruded LA51 alloy is owing to both smaller yield ratio and larger n-value.

Besides, the formability of Mg alloy has a strong relationship with the texture. According to the results reported by Chino *et al.*², it may be caused by the thickness-direction strain under different tensile stress. The thickness-direction strain was often observed under biaxial tensile stress. The outstanding stretch formability of the extruded LA51 sheet was on account of the reinforcement of thickness-direction strain due to the weak basal texture. As a consequence, it is a proven and effective method of enhancing mechanical properties and formability of magnesium alloy at room temperature, that alloying with lithium and two-pass extrusion.

4 Conclusions

The microstructure, texture evolution and mechanical properties of two-pass extruded Mg-5Li-1Al alloy have been investigated. The following conclusions can be drawn: Two-pass extrusion is developed to refine the grains of LA51 alloy, and uniform microstructure can be obtained. α -Mg phase is the only constituents of the two-pass extruded sheet. The dynamic recrystallization can occur more sufficient in two-pass extrusion. The two-pass extruded LA51 sheet shows a weak basal texture with basal pole tilting towards TD and accordingly improved the ductility and formability. The good mechanical property and formability are attributed to lithium addition and dynamic recrystallization during two-pass extrusion.

Acknowledgement

This study was supported by natural science foundation of the Inner Mongolia autonomous region

(Nos, 2019MS05037, 2015BS0512), and the “Chunhui Plan” Cooperative Research Projects of China Ministry of Education (No.CHJH2018), and Inner Mongolia University of Science and Technology Innovation Fund (No.2014QDL016).

References

- 1 Karakulak E, *J Magn Alloy*, 7 (2019) 355.
- 2 Chino Y, Sassa K & Mabuchi M, *Mater Sci Eng A*, 513–514 (2009) 394.
- 3 Liu F, Guo C, Xin R, Wu G & Liu Q, *J Magn Alloy*, 7 (2019) 258.
- 4 Cho DH, Nam JH, Lee BW, Cho KM & Park IM, *J Alloys Compd*, 676 (2016) 461.
- 5 Das SK, Brodusch N, Gauvin R & Jung I-H, *Scr Mater*, 80 (2014) 41.
- 6 Dong H, Pan F, Jiang B & Zeng Y, *Mater Des*, 57 (2014) 121.
- 7 Hauser FE, Landon PR & Dorn JE, *Trans ASM*, 50 (1958) 856.
- 8 Hooper R-M, Bryan Z & Manuel M, *Metall Mater Trans A*, 45 (2014) 55.
- 9 Jiang LY, Zhang DF, Fan XW, Guo F, Xue HS & Pan FS, *Mater Sci Technol*, 32 (2016) 1.
- 10 Kim Y-H, Kim J-H, Yu H-S, Choi J-W & Son H-T, *J Alloys Compd*, 583 (2014) 15.
- 11 Xu T, Yang Y, Peng X, Song J & Pan F, *J Magn Alloy*, 7 (2019) 536.
- 12 Lee C, Koh Y, Seok D-Y, Kim H, Lee M-G & Chung K, *Int J Mater Form*, 9 (2014) 287.
- 13 Li C, Tan H & Wu WM, *Mater Sci Technol*, 32 (2016) 1.
- 14 Li R, Pan F, Jiang B, Yang Q & Tang A, *Mater Des*, 46 (2013) 922.
- 15 Li X, Wang F, Li X, Zhu J & Tang G, *Mater Sci Technol*, 32 (2016) 1.
- 16 Zhang T, Tokunaga T, Ohno M, Wu R, Zhang M & Matsuura K, *Mater Sci Eng A*, 737 (2018) 61.
- 17 Liu X, Wu R, Niu Z, Zhang J & Zhang M, *J Alloys Compd*, 541 (2012) 372.
- 18 Mackenzie LWF & Pekguleryuz M, *Mater Sci Eng A*, 480 (2008) 189.
- 19 Meng F, Rosalie JM, Singh A, Somekawa H & Tsuchiya K, *Scr Mater*, 78–79 (2014) 57.
- 20 Ning ZL, Yi JY, Qian M, Sun HC, Cao FY, Liu HH & Sun JF, *Mater Des*, 60 (2014) 218.
- 21 Park GH, Kim JT, Park HJ, Kim YS, Jeong HJ, Lee N, Seo Y, Suh J-Y, Son H-T, Wang W-M, Park JM & Kim KB, *J Alloys Compd*, 680 (2016) 116.
- 22 Son H-T, Kim Y-H, Kim D-W, Kim J-H & Yu H-S, *J Alloys Compd*, 564 (2013) 130.
- 23 Styczynski A, Hartig C, Bohlen J & Letzig D, *Scr Mater*, 50 (2004) 943.
- 24 Suh B-C, Shim M-S, Shin KS & Kim NJ, *Scr Mater*, 84–85 (2014) 1.
- 25 Wang BJ, Xu DK, Dong JH & Ke W, *Scr Mater*, 88 (2014) 5.
- 26 Yun Y, Cai Q, Xie B & Li S, *J Iron Steel Res Int*, 24 (2017) 950.
- 27 Wang L, Li JB, Li L, Nie KB, Zhang JS, Yang CW, Yan PW, Liu YP & Xu CX, *Mater Sci Technol*, 32 (2016) 1.
- 28 Xin R, Zheng X, Liu Z, Liu D, Qiu R, Li Z & Liu Q, *J Alloys Compd*, 659 (2016) 51.
- 29 Yang Q, Jiang B, Li J, Dong H, Liu W, Luo S & Pan F, *Int J Mater Form*, 9 (2015) 305.
- 30 Agnew S & Duygulu Ö, *Int J Plasticity*, 21 (2005) 1161.
- 31 Alaneme K & Okotete E, *J. Magnes. Alloy*, 5 (2017) 460.
- 32 Zeng Y, Jiang B, Yang Q, Quan G, He J, Jiang Z & Pan F, *Mater Sci Eng A*, 700 (2017) 59.
- 33 Zhong L, Peng J, Li M, Wang Y, Lu Y & Pan F, *J Alloys Compd*, 661 (2016) 402.
- 34 Zhou L, Su K, Wang Y, Zeng Q & Li Y, First-principles study of the properties of Li, Al and Cd doped Mg alloys. *J Alloys Compd*, 596 (2014) 63.
- 35 Zhu T, Sun J, Cui C, Wu R, Betsofen S, Leng Z, Zhang J & Zhang M, *Mater Sci Eng A*, 600 (2014) 1.
- 36 Kang D, Kim D, Kim S, Bae G, Kim K & Kim N, *Scr Mater*, 61 (2009) 768.